



Characteristics of boundary plasmas after the removal of divertor baffle plates and boronization on JFT-2M

H. Kawashima ^{*}, S. Sengoku, K. Tsuzuki, H. Ogawa, H. Kimura

Tokai Annex, Naka Fusion Research Establishment, Japan Atomic Energy Research Institute, Tokai, Naka, Ibaraki 319-1195, Japan

Abstract

A dense and cold divertor ($n_e^{\text{div}} \sim 2 \times 10^{19} \text{ m}^{-3}$, $T_e^{\text{div}} \sim 6 \text{ eV}$) during H-mode, was realized with the closed divertor (CD2) on JFT-2M. By removing all baffle plates, such a condition was compared between open (OD) and closed configurations. When a strong gas-puff is introduced into the divertor region during L-mode, the baffling effect of CD2 is verified definitely by the reduction of neutral particle backflow and the enhanced radiation localization in the divertor region. Introducing a strong gas-puff during H-mode for the OD case, H-mode is terminated in an early stage when the radiation loss fraction exceeds a critical level. A dense and cold divertor, as shown in the CD2 case, is not obtained. This is attributed to the lack of particle-handling capability for the OD compared with the CD2 configuration. As an initial result, the radiation loss fraction was reduced by half after the boronization which prevents the H-L transition.

© 2003 Elsevier Science B.V. All rights reserved.

PACS: 52.55.Fa

Keywords: Open and closed divertor; Dense and cold divertor; Strong gas-puff; Baffling effect; H-mode; Boronization

1. Introduction

The divertor of a fusion reactor is required to minimize the heat load onto the divertor targets while keeping high core confinement, as the machine size should be reasonably compact for a future reactor. Remote radiative cooling by fuelling or impurity gas-puff in the divertor chamber is one of the reduction methods of the heat load. However, the quality of core plasma confinement was adversely affected by a backflow of neutral particles from the divertor to the main plasma region [1]. To prevent this, the divertor configuration has been structurally modified with baffle plates in some tokamak machines [2]. Although the plasma configurations and control were relatively limited by the baffle plates, a more tightly baffled closed-divertor (CD2) [3,4] was adopted in the JFT-2M ($R = 1.31 \text{ m}$, $a = 0.35 \text{ m}$,

$\kappa \leq 1.7$, $B_t \leq 2.2 \text{ T}$) in order to increase the particle-handling capability. With this configuration, a dense and cold divertor state ($n_e^{\text{div}} \sim 2 \times 10^{19} \text{ m}^{-3}$, $T_e^{\text{div}} \sim 6 \text{ eV}$) with an ELM free H-mode was realized by a strong gas-puff in the divertor chamber [5].

In order to clarify the degree of particle-handling capability of the CD2, the divertor configuration was modified to an open divertor (OD) configuration by removing all of the baffle plates. By introducing a strong gas-puff into the divertor region in L-mode or H-mode plasmas similar to the CD2 case, the difference of particle-handling capability between the CD2 and the OD was examined. In order to reduce the impurity influx and to minimize the radiation loss power that terminates the H-mode when enhanced over a critical level, a boronization [6,7] system was installed in JFT-2M [8].

In Section 2, the modification of the CD2 to the OD and the boronization system are described. The baffling effect of the closed divertor configuration is shown in Section 3. Section 4 presents the characteristics of divertor and core plasmas for the OD configuration during an ELM free H-mode with a strong gas-puff. The

^{*} Corresponding author. Tel.: +81-29 282 5468; fax: +81-29 282 5614.

E-mail address: kawasimh@fusion.naka.jaeri.go.jp (H. Kawashima).

dense and cold divertor state in the OD case was not obtained due to H-mode termination by the abrupt increase of radiation loss power. An initial result of the boronization, which reduces the radiation loss power remarkably, is shown in Section 5. Conclusions are given in Section 6.

2. Modification of closed divertor to open divertor

The divertor configuration in the lower part of JFT-2M was modified from the closed divertor (CD2) to the open divertor (OD) configuration as shown in Fig. 1. The divertor and baffle plates are made of stainless steel (SS) and are toroidally continuous for the CD2. For the OD, all baffle plates on inside, outside and private regions are removed and the continuous SS divertor plates are retained. This modification enables us to compare open- and closed-divertor plasma characteristics with same lower-single-null (LSN) configuration. The upper side was kept as an open divertor configuration with discrete graphite divertor plates.

After the series of the divertor experiments, boronization was carried out with DC glow discharge in a mixture gas of 1% tri-methyl-boron (TMB: $B(CH_3)_3$) and

99% He. It was confirmed that boron films of ~ 100 nm were deposited on almost the whole inner surface of the vacuum vessel [8].

The electron temperature and density of the divertor plasmas are measured by embedded Langmuir probes on the divertor plates. A bolometer is used to measure the total radiation loss power from the main plasma. The radiation profile is measured by using both horizontal and vertical bolometer array systems in the divertor and main plasma regions. H-mode plasmas are obtained by hydrogen neutral beam injection (NBI) with power up to 800 kW. The working gas is deuterium.

3. Verification of the baffling effect for the closed divertor configuration

In order to verify the degree of neutral particle or impurity shielding by baffle plates for the CD2, the plasma performance was compared between the CD2 and OD configurations with a strong gas-puff into the divertor region. Fig. 2 shows the time evolution of plasma parameters with a divertor gas-puff Q^{div} of $3 \text{ Pa m}^3/\text{s}$, which is several times larger than that of the normal operation, during a steady state L-mode (co-NBI, 600 kW) for both CD2 (solid lines) and OD (broken lines)

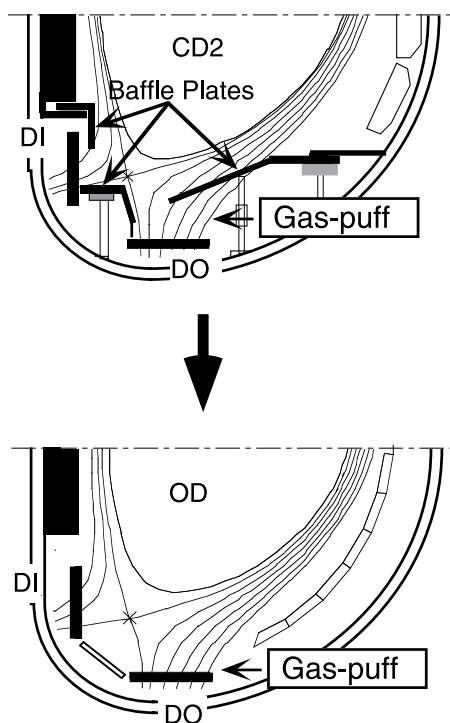


Fig. 1. Schematic view of previous closed divertor (CD2) and modified open divertor (OD) in the JFT-2M tokamak.

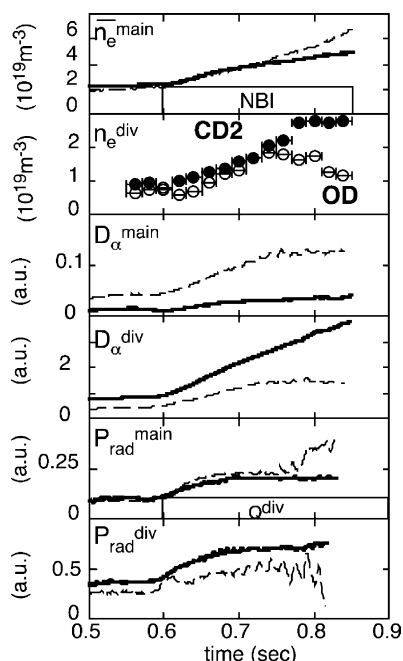


Fig. 2. Time evolution of plasma parameters with application of a divertor gas-puff $Q^{div} = 3 \text{ Pa m}^3/\text{s}$ for the CD2 (solid lines) and the OD (broken lines) with L-mode plasmas. $I_p = 230 \text{ kA}$, $B_t = 1.3 \text{ T}$ (CCW), and the LSN divertor configuration are used.

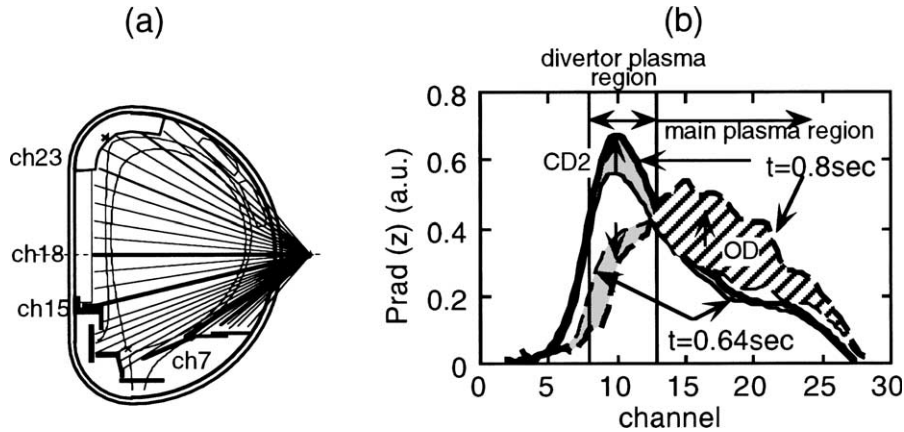


Fig. 3. (a) Viewing chords of horizontal bolometer array. The bolometers of channels 8–13 view the lower divertor region, and those of channels 14–27 view the main plasma region. (b) Horizontal profiles of radiation loss at $t = 0.64$ and 0.80 s in Fig. 2 for CD2 and OD cases.

(broken lines) cases. In these cases, the plasma current I_p is 230 kA, the toroidal field B_t is 1.3 T, and the safety factor is ~ 3 with a LSN configuration. The B_t direction is in the counter clockwise (CCW) direction in order to avoid an H-mode transition and obtain L-mode plasmas with higher power. For the CD2, the increments of main plasma density \bar{n}_e^{main} and peripheral light emission of deuterium in the main plasma side D_α^{main} are 70% and 50% of those for the OD case, respectively. Whereas, the increments both of divertor electron density, n_e^{div} , and light emission, D_α^{div} , (both are experimentally roughly proportional to the neutral pressure in the divertor chamber) are 2.5 times as large as that of OD case. These changes indicate the reduction of neutral particle back-flow from the divertor region to main plasma peripheral region by the baffle plates for the CD2. There is also contrastive behavior for radiation loss for main and divertor region ($P_{\text{rad}}^{\text{main}}$ and $P_{\text{rad}}^{\text{div}}$) between OD and CD2 cases as shown in the bottom two boxes in Fig. 2. $P_{\text{rad}}^{\text{main}}$ and $P_{\text{rad}}^{\text{div}}$ for CD2 are lower and higher than those for OD, respectively, and their gap expands remarkable after $t \sim 0.75$ s. Fig. 3(b) shows the horizontal profiles of radiation loss by the bolometer array. The viewing chord of each bolometer channel is shown in Fig. 3(a). The enhancement of the radiation loss from $t = 0.64$ – 0.80 s is indicated by the shading in the figure. The main part of the radiation loss is moved from the divertor to the main plasma regions in the OD case. Whereas the enhancement of radiation loss is localized only in the divertor region in the CD2 case. It is suggested that radiation enhancement in the main plasma region for the OD case is due to the increment of impurity influx. The enhanced radiation localization in the divertor region for CD2 case seems to be dominated by a strong buildup of electron density near the divertor plate since radiation loss is also proportional to the electron den-

sity. It is attributed to the existence of baffle plates, which also leads to high particle recycling in the divertor chamber, low particle recycling around the main plasma edge and low core fuelling.

4. Effect of a strong gas-puff during an ELM free H-mode for the OD configuration

It was shown that strong gas puffing prolonged the ELM free H-mode duration, and an effective dense and cold divertor state was obtained during the H-mode with the CD2 configuration [9]. For the open divertor configuration after removing all baffle plates, similar experiments were carried out to make clear the difference between both divertor configurations.

Fig. 4 shows the time evolution of the total radiation loss fraction to the input power $P_{\text{rad}}^{\text{total}}/P_{\text{in}}$, main plasma density, \bar{n}_e^{main} , and light emission, D_α^{main} , and divertor electron temperature, T_e^{div} , and density, n_e^{div} , for the cases without and with a gas-puff during the ELM free H-mode. An ELM free H-mode is obtained by 800 kW co-NBI heating. The H-mode duration of 72 ms (Fig. 4(a): without gas-puff) is shortened to 60 ms by a strong gas-puff of $Q^{\text{div}} = 3.3 \text{ Pa m}^3/\text{s}$ (Fig. 4(b)). The H-mode is terminated critically at the radiation fraction level of $P_{\text{rad}}^{\text{total}}/P_{\text{in}} \sim 0.6$ for both cases similar to the upper-single-null (USN) open divertor [3]. By gas puffing, the increment of $P_{\text{rad}}^{\text{total}}/P_{\text{in}}$ is enhanced abruptly ($\Delta(P_{\text{rad}}^{\text{total}}/P_{\text{in}})/\Delta t$ becomes ~ 1.8 times larger than that without gas-puff), which might be a cause of the shortened H-mode duration. For that period, a decrease of T_e^{div} and increment of n_e^{div} are observed, but they are at a standstill $\geq 10 \text{ eV}$ and $\leq 0.6 \times 10^{19} \text{ m}^{-3}$, respectively.

In Fig. 5(a)–(c), the divertor electron density and temperature and the enhancement factor of the global

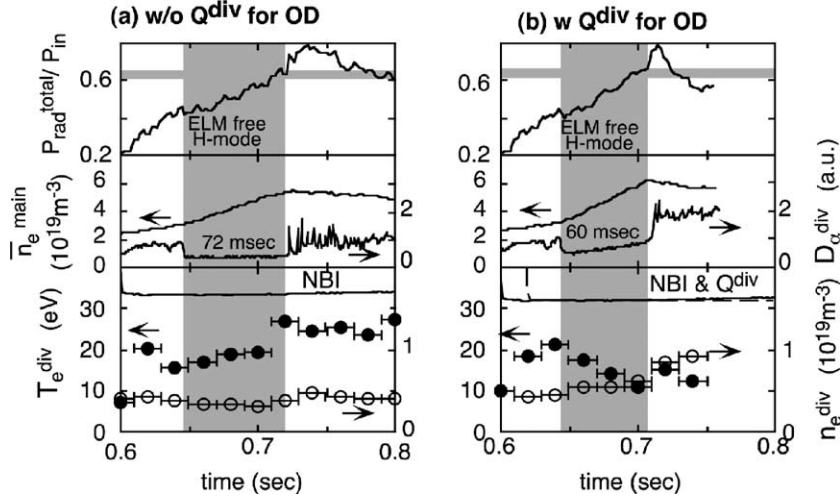


Fig. 4. Time evolution of plasma parameters for OD (a) without and (b) with gas puff during an ELM free H-mode obtained by 800 kW NBI. I_p , B_t and plasma configuration are the same as in Fig. 2 except for the clockwise B_t direction.

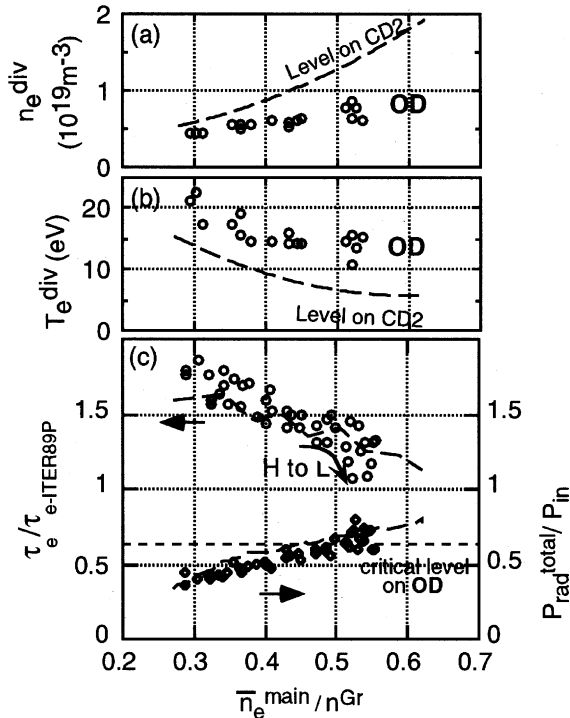


Fig. 5. Divertor electron density and temperature, and the enhancement factor of the global energy confinement time $\tau_E/\tau_{E-ITER89P}$ during ELM free H-mode as a function of the main plasma density normalized by the Greenwald density limit $\bar{n}_e^{\text{main}}/n^{\text{Gr}}$ for the OD configuration. Broken lines show the previous CD2 level.

energy confinement time $\tau_E/\tau_{E-ITER89P}$ [10] during the ELM free H-mode are summarized as a function of the main plasma density normalized by the Greenwald

density limit [11] $\bar{n}_e^{\text{main}}/n^{\text{Gr}}$ for OD. When $\bar{n}_e^{\text{main}}/n^{\text{Gr}}$ is increased by a strong gas-puff, n_e^{div} increases up to $1 \times 10^{19} \text{ m}^{-3}$ and T_e^{div} decreases and then saturates above 10 eV. However, they never reach the level of the CD2 as shown by the broken lines. The $\tau_E/\tau_{E-ITER89P}$ of an ELM free H-mode plasmas decreases continuously from ~ 1.8 to ~ 1.3 with increasing density. Afterward H- to L-mode transition occurs when $P_{\text{rad}}^{\text{total}}/P_{\text{in}}$ is enhanced and exceeds a critical level ~ 0.6 at $\bar{n}_e^{\text{main}}/n^{\text{Gr}} \sim 0.53$. Thus, it was shown that the divertor plasma state obtained with a strong gas-puff with an ELM free H-mode is inferior to that for the CD2, due to the $P_{\text{rad}}^{\text{total}}/P_{\text{in}}$ exceeding a critical level at an early stage in the OD configuration.

5. Reduction of radiation loss power by boronization

It can be expected from above results that the H-mode duration could be prolonged and the dense and cold divertor progresses further by minimizing the radiation loss power. This might not be a neutral particle problem, but an impurity problem. Boronization was applied to reduce this radiation loss power. As an initial result, $P_{\text{rad}}^{\text{total}}/P_{\text{in}}$ before and after boronization as a function of \bar{n}_e^{main} is shown in Fig. 6. This experiment was performed at a limiter configuration with $I_p = 200 \text{ kA}$, $B_t = 1.3 \text{ T}$ for ohmic plasmas. Before boronization, the radiation loss power was as high as 65% of the ohmic heating power; it is reduced successfully by a factor of 2 after the boronization. The oxygen emission also reduced by a factor of 10 after the boronization. For H-mode plasmas with USN divertor configuration without divertor gas-puff, $P_{\text{rad}}^{\text{total}}/P_{\text{in}}$ was kept low, under the critical level and the H-mode was not terminated during

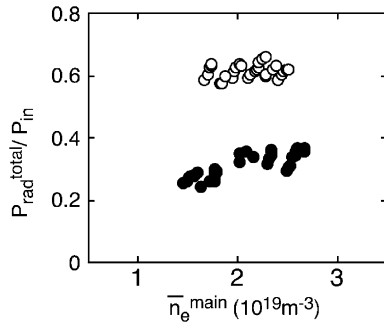


Fig. 6. Radiation loss fraction $P_{\text{rad}}^{\text{total}}/P_{\text{in}}$ before (open circles) and after (closed circles) boronization as a function of $\bar{n}_{\text{e}}^{\text{main}}$ for ohmic plasmas with a limiter configuration. Here P_{in} is ohmic input power.

the heating phase (200 ms). Hereafter, boronization is counted on for the study of dense and cold divertor with higher density and higher confinement.

6. Conclusions

The plasma performance associated with a strong gas-puff into the divertor region was compared with the open (OD) and closed (CD2) divertor configurations. The baffling effect of the CD2 is verified definitely by the reduction of neutral particle backflow and the enhanced radiation localization in the divertor region in L-mode plasmas with a strong gas-puff. The reduction of neutral particle backflow is shown typically from the 50% reduction of D_{α} emission in the main plasma periphery and the increment of D_{α} emission in the divertor region by a factor of 2.5. When a strong gas-puff is introduced during an ELM free H-mode for the OD case, the H-mode is terminated in the early stage by an abrupt increase of the radiation loss power reaching the critical level. The obtained divertor plasma ($n_{\text{e}}^{\text{div}} \leq 1 \times 10^{19} \text{ m}^{-3}$, $T_{\text{e}}^{\text{div}} \geq 10 \text{ eV}$) in H-mode at $\bar{n}_{\text{e}}^{\text{main}}/n^{\text{Gr}} \sim 0.5$ is inferior to that of the dense and cold divertor state in CD2. These

are attributed to the lack of particle-handling capability for the OD compared with the CD2 configuration. As an initial result, the radiation loss fraction is reduced by half after the boronization which prevents the H–L transition. It is counted on for the future study of a dense and cold divertor with higher density and higher confinement.

Acknowledgements

The authors are much indebted to the JFT-2M group for support with the experiments and capable operation. Thanks are also due to Drs A. Kitsunezaki, M. Kikuchi and Y. Kusama for continuous encouragement.

References

- [1] N. Asakura, K. Shimizu, H. Shirai, et al., Plasma Phys. Control. Fusion 39 (1997) 1295.
- [2] ITER Physics Basis, Nucl. Fusion 39 (1999).
- [3] S. Sengoku, H. Kawashima, and JFT-2M Group, Bull. Amer. Phys. Soc. 42 (1997) 1962.
- [4] H. Ogawa, Y. Miura, N. Fukumoto, et al., J. Nucl. Mater. 266–269 (1999) 623.
- [5] H. Kawashima, S. Sengoku, T. Ogawa, et al., Nucl. Fusion 39 (1999) 1679.
- [6] C. Skinner, H. Kugel, R. Maingi, et al., Nucl. Fusion 42 (2002) 329.
- [7] O. Buzhinskij, Y. Semenets, Fus. Technol. 32 (1997) 1.
- [8] K. Tsuzuki, M. Sato, H. Kawashima, et al., Proc. 11th Int. Conf. On Fusion Reactor Materials, Baden-Baden, 2001.
- [9] H. Kawashima, S. Sengoku, T. Ogawa, et al., Controlled Fusion and Plasma Physics, (Proc. 24th Eur. Conf. Berchtsgaden, 1997), vol. 21A, Part II, European Physical Society, Geneva, 1997, p. 705.
- [10] P. Yushmanov, T. Takizuka, K. Riedel, et al., Nucl. Fusion 30 (1990) 1999.
- [11] M. Greenwald, J. Terry, S. Wolfe, et al., Nucl. Fusion 28 (1988) 2199.